Journal of Advances and Scholarly Researches in Allied Education
Vol. 13, Issue No. 1, April-2017, ISSN 2230-7540

Elastic Scattering and Aggregate Response Cross Segment with Radioactive Ion Beam

Deepak Saini[1]* Dr. Anil Kumar[2]

[1] Research Scholar of OPJS University, Churu, Rajasthan

[2] Associate Professor, OPJS University, Churu, Rajasthan

Abstract – In the present work we examine add up to response cross areas for an assortment of frameworks comprising on feebly, firmly bound and radioactive proton or neutron corona shots on light targets. It is along these lines intriguing to explore whether its aggregate response cross-area on various targets carries on more get a kick out of the chance to responses initiated by 8B reflect or to the steady isotopes 6Li and 7Li, as there were not very numerous information accessible for responses actuated by this shot in writing. There are just a single vitality point estimation accessible for the 8Li + 51V framework and two vitality point estimations accessible for the 8Li + 9Be framework. Also, there is a wide vitality hole of 13 MeV between the prior estimations in the 8Li + 9Be framework. In this way, we have estimated some additional versatile dispersing rakish conveyances for the 8Li + 9Be and 8Li + 51V frameworks at the occurrence energies, 19.6 MeV and 18.5 MeV, individually, with the end goal to supplement the present information with the past trial information.

Keywords: Elastic Scattering, Aggregate Response, Cross Segment, Radioactive, Ion Beam.

---------------------------------x---------------------------------

INTRODUCTION

It is notable that the properties of cores a long way from the steadiness valley contrast in numerous angles from those of normal cores [1-9]. The idiosyncrasies of atomic powers and many-body frameworks make plausible the presence of both light and overwhelming feebly bound cores with a diffuse surface layer. The relationships of the valence neutrons and the solid coupling with the continuum can fundamentally mutilate the shell structure and also the aggregate properties of the pitifully bound unbalanced cores with N > Z. Impacts because of these properties ought not out of the ordinary likewise in the elements of the responses prompted by these cores. With the enhancement of radioactive particle pillar (RIB) quickening methods, it has turned out to be conceivable to create variable vitality, generally extraordinary light emissions cores in an extensive variety of N and Z. The utilization of optional light emissions cores impressively broadens the potential outcomes to examine the properties of nuclear cores and atomic responses. There are three primary issues of atomic material science to be tended to in the trials including fleeting radioactive particle shafts: the examination of the properties of the nuclear cores a long way from the security line, the investigation of the quirks of the elements of atomic responses actuated by proton-and neutron-rich cores and the blend and properties of new components and isotopes.

The low-vitality responses of few-nucleon exchange instigated by radioactive shafts open up new potential outcomes to examine the group structure and to get the spectroscopic qualities of brief cores [10-12]. Additionally of incredible intrigue are some different responses system incited by radioactive cores, for example, flexible dispersing, combination and separation. These response instruments are firmly corresponded and give new data both on the structure of the feebly bound cores and on the atomic elements in which they take an interest. The versatile disseminating of light fascinating cores gives data on the core cooperation of frameworks a long way from steadiness, which are portrayed by substantial isospin and solid coupling to the continuum, to be specific the separation channel of the pitifully bound core. The parameters of this cooperation are of intrigue independent from anyone else, as well as they are vital for examination and comprehension of the elements of more confounded responses .

It is of extensive enthusiasm to consider the versatile disseminating on light, medium and overwhelming focuses on that assume a main job towards the comprehension of the separation of the feebly bound frameworks. From this, it is imperative to examine the flexible diffusing on various shot target blends with changing asymmetry, with the end goal to see more muddled responses. The cross-area of flexible dissipating can get an optical potential which is important to comprehend the passageway and leave channel possibilities of some exchange responses. Separation impacts additionally assume a vital job in the disseminating system, influencing the cooperation potential. One of the critical purposes of examination is whether the impact of separation is basically to expand the aggregate response cross-segment. In this way, it is essential to research the reliance of the separation and aggregate response cross-segments on the separation limit for various shots on light-and medium-mass targets.

For an efficient investigation of response cross-areas, an immediate examination of information with hypothetical forecasts for every framework isn't extremely advantageous since various frameworks would be twisted by contrasts like the shot's charge or/and estimate. It is then important to lessen the information in a way that the impact of such factors would be washed out. For this reason, diverse recommendations can be found in the writing. A couple of years prior a decrease strategy was recommended that has been generally utilized [19]. Notwithstanding, as of late another decrease methodology was proposed [20] for the investigation of combination of pitifully bound cores and later reached out to add up to response cross-segments [13] . These strategies prompt by one way or another distinctive outcomes for a few shots on the 27Al target [13, 21]. In the present work we look at the outcomes utilizing both the techniques for the frameworks examined, to be specific, 8Li + 9Be,51V.

Details of Radioactive Ion Beam Production

The try different things with radioactive bar exhibited in this part were performed in the framework RIBRAS [22, 23] (Radioactive Ion Beams in Brazil), at University of Sao Paulo, Sao Paulo, Brazil (Fig. 5.1). This contraption is proportional to TwinSol [24] at the lab of Notre Dame. RIBRAS framework comprises of a couple of superconducting solenoids that are fit for isolating particles and deliver light emissions cores. The portrayal of the profile of optional shafts created in RIBRAS was made utilizing an indicator PPAC (parallel plate torrential slide counter) [25].

1. Radioactive Beams

Extraordinary cores can be contemplated with the utilization of auxiliary pillars. The force and immaculateness of these shafts are relative and differ as indicated by the identity of each test. When all is said in done, a force more noteworthy than 104 particles/s is adequate to work, and an auxiliary pillar debased, even with numerous contaminants, it is worthy on the off chance that they don't meddle in the aftereffects of intrigue. There are a few conceivable techniques for the creation of radioactive bars [26]. By and large there exist two corresponding approaches to make great quality light emissions cores: (I) the in-flight detachment system and (ii) the isotope partition on line (ISOL) method. A driver quickening agent or reactor gives the particles inciting atomic responses in an objective. In the in-Flight strategy the essential particles must be overwhelming and vigorous and the objective must be thin with the end goal to have the response items pulling back out of the objective (splitting is an exemption to the announcement of substantial and lively particles as the response likewise can be initiated by photons, electrons and light particles; the vitality discharged in parting is sufficiently high for the sections to leave the thin target). The In-Flight technique is pertinent to short-living cores (ps) as just the flight time from the creation focus to the estimating station instigates rot misfortunes. With the In-Flight technique the radioactive particles are vivacious and can in the end be backed off and put away. In the ISOL technique the radioactive items must be thermalized in a catcher and after that reaccelerated. The subsequent bars are particle optically (emittance, vitality goals, timing structure) of fantastic quality however the thermalization procedure and the inevitable re-ionization in the particle source can be moderate and even wasteful prompting serious misfortunes for short-living cores or for isotopes from recalcitrant components. In the event that the backing off process occurs in a vaporous catcher leaving the particles in a 1+ charge state (in the end after re-ionization by thunderous laser light), these lacks of the objective catcher-particle source frameworks in the regular ISOL can be stayed away from. This is likewise the way how the best of both (In Flight and ISOL) universes can be gotten and an excellent light emission living radioactive particles can be created.

The method utilized for the creation of radioactive bars in the framework RIBRAS, is the move of nucleons in flight. The strategy empowers the generation of valuable cores with short half life (T1/2 » 100ns) and low vitality (3-5MeV/u in the present get together of RIBRAS after the Pelletron quickening agent). In this procedure, an essential light emission vitality centers around an objective of creation (additionally called the essential focus on) that will deliver an auxiliary light emission cores by exchange responses (a couple of nucleons) with extensive cross segments. The radioactive particles are then isolated by attractive fields (if the RIBRAS) and/or electric. In spite of

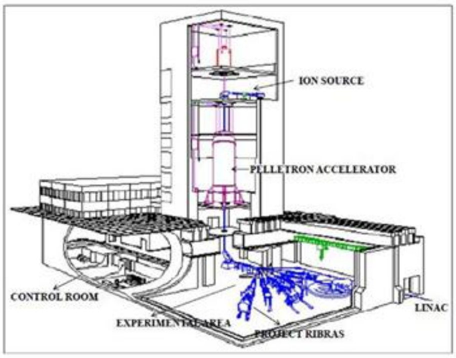

Figure 5.1: Overview of the Pelletron Laboratory of the Institute of Physics of the University of Sao Paulo, Brazil, RIBRAS system.

ION SOURCE

The wellspring of particles MC-SNICS (Multi Cathode - Source of Negative Ions by Cesium Sputtering), worked by National electrostatics Corporation (NEC), produces light emissions particles or atoms. With the end goal to acquire light emissions and 7Li, material containing these concoction components and arranged, stored and compacted in extraordinary pots of about 1mm in measurement, which are called cathodes. This source permits the get together of up to 32 distinctive cathode materials, enabling the change starting with one bar then onto the next rapidly and without the need to open the source and uncover the air cathode. The yield pillar at the source is given by cesium particle barrage of the material stored on the cathode . The cesium vapor, shaped in the "warming" (compartment warmed to 120 °C), enters through a valve in a zone (ionization chamber) between the cathode and a chilly surface ionizing warmer (the ionizer).

A segment of the cesium is dense on the surface of the cathode material and another part is emphatically ionized by ionizer surface. The cesium ionized particles are quickened toward the cathode, crashing into the particles of the material which are catapulted (sputtering). A few materials radiate negative particles, while others remove impartial or decidedly charged particles. The last catches the valence electrons of cesium dense layer on the surface of the material, delivering a light emission particles. This pillar is then extricated from the source through a capability of 20 kV extractor. The bar current acquired in a Faraday container for 7Li ran from 200 nA to 400 nA and for 6Li was kept up at around 800 nA to 1pA.

Pelletron Accelerator

Not long after leaving the pre-quickening agent tube, the pillar contains an assortment of particles created at the source, of which just a single is wanted, for this situation, Li. The particles are chosen by their mass (M), vitality (E) and charge (Z) by the activity of an electromagnet whose greatest esteem is ME/Z which is 20 (ME-20), which avoids the shaft 90°, abandoning it upstanding and guiding it to the terminal of the quickening agent.

The 8 UD Pelletron quickening agent is an electrostatic machine, Tandem type with 8 MeV greatest voltage at the terminal. The charge of the terminal is delivered by activity on the inductive current of metallic chambers (pellets) with protecting nylon joins. A high voltage supply spellbinds a negative inductor grounded close to the pulley; this drives the electrons out of the pellets as they are in contact with the pulley. Since the pellets stay on the activity of the field of the inductor while leaving the pulley, they store a measure of positive charge.

RIBRAS

The RIBRAS is a framework made out of two superconducting solenoids introduced in the pipe 45-B Pelletron-LINAC research facility of Sao Paulo University, Brazil, that permits in-flight creation of optional light emissions radioactive cores of low (vitality of the auxiliary pillar 2-10 MeV/u). This device (Fig. 5.3) is equipped for creating a wide assortment of light pillars, for instance: 8Li, 6He, 7Be, 8B and 18mF, with powers going from 104-106 pps.

The initial phase in delivering an optional shaft is the frequency of the essential pillar on an objective (essential target), creating the coveted response. The essential target is in the focal point of the objective chamber, around one meter from the focal point of the main solenoid. The framework RIBRAS has a gas framework that permits the utilization of targets or just cooling gas to strong targets. Havar sheets are utilized to seal the windows for section and exit of the objective. The essential targets are installed in the strong yield window, keeping the passage window shut with a fixing sheet Havar. The cooling is normally finished with helium gas, which should be possible with air at a higher expense of vitality corruption. Table 5.1 gives a rundown of models of exchange responses to create cores a long way from dependability line:

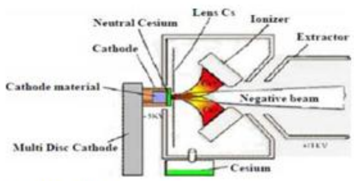

Reservoir
Figure 5.2: Schematic diagram of the sputtering process.

Figure 5.3: RIBRAS solenoid and target system for the production of radioactive ion beams.

Table 5.1 Possible radioactive ion beams obtained from the system RIBRAS.

Radioactive beam	Production reaction
^{8}Li	^{9}Be(^{7}Li,^{8}Li)^{9}Be [31]
^{6}He	^{9}Be(^{7}Li,^{6}He)^{10}B [31]
^{7}Be	^{3}He(^{6}Li,^{7}Be)d [31]
^{7}Be	^{3}He(^{7}Li,^{7}Be)t
^{8}B	^{3}He(^{6}Li,^{8}B)n
^{12}B	^{9}Be(^{7}Li,^{4}He)^{12}B [31]
18mF	^{12}C(^{17}O,^{18m}F)^{11}B [31]

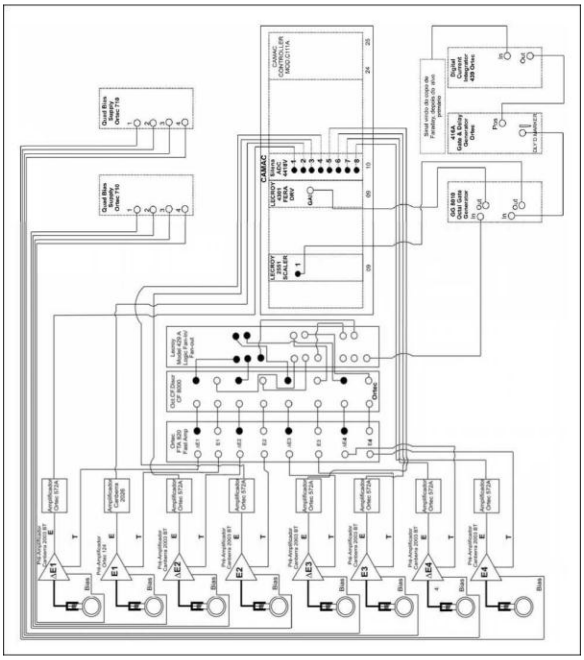

Figure 5.4: Electronics used in data acquisition.

ELECTRONICS AND DATA ACQUISITION

The electronic get together utilized in the analyses can be found in Fig. 5.4. The voltage identifier is provided from two sources Quad Bias Supply ORTEC 710. The beats created by the silicon surface hindrance finders experience pre-intensifiers (models 142 PC-ORTEC and Canberra 2003BT), simply outside the dissipating chamber. The signs of the power yields of the preamplifiers are sent to intensifiers ORTEC 572A, where the gain is balanced and frame (shapping time) of the bipolar heartbeats sent to the simple to advanced converter (ADC 4418V-SILENA) of CAM AC (Computer Automated Measurement and Control/Model C111A) for further information handling.

The time signals are sent to a quick speaker (ORTEC 820-FTA Fast Amp) and after that changed into a rationale flag discriminator module Octal CF 8000 ORTEC. A rationale module Fan in/Fan out gets the signs from all finders creating a solitary flag at its yield, which is transmitted to a module OGG demonstrate - ORTEC module GG8010. The OGG creates a rationale flag that fills in as a trigger for the CAMAC framework, cautioning of the event of occasions. Amid this period, the CAMAC keeps the perusing of unipolar heartbeats for ADC's and after that forms them with the assistance of the module EH , recently customized by the User.

The perusing of the Faraday glass is shaped by a present integrator (Digital Current Integrator ORTEC-429), changed into legitimate heartbeats (416A Gate and Delay Generator-ORTEC) set in OGG and gained by the scalar (LECROY, 2551) of CAMAC. The information is at long last sent to the information obtaining framework (Scan Root-Linux), which notwithstanding controlling the CAMAC is in charge of chronicle the information in the microcomputer procurement radioactive particle bar 8Li was delivered with the RIBRAS (Radioactive Ion Beams in Brazil) framework [16, 21, 28, and 29]. Versatile dispersing precise conveyances and the comparing all out response cross-areas were accessible in the writing for one vitality (Elab = 26 MeV) for the 8Li + 51V framework [29] and two energies (14 MeV and 27 MeV) [18, 32] for the 8Li + 9Be framework. As there are extensive vulnerabilities in the aggregate cross¬sections got from the flexible diffusing of radioactive cores, it is vital to acquire more information to have the capacity to incorporate these frameworks in the efficient. The depiction of the generation of radioactive particle pillars utilizing the RIBRAS office has been talked about somewhere else [16, 21, 28, and 29]. The 8Li radioactive particle bar was created utilizing an essential neutron exchange response 9Be (7Li, 8Li). The thickness of the essential target 9Be is of 12 mg/cm2, which is mounted in a disseminating chamber just before the main solenoid. The essential pillar 7Li was quickened with an ordinary shaft power of 200 nAe, estimated by utilizing an electron-smothered Faraday glass, comprised by a disconnected tungsten pole that stops every one of the particles in the precise area from 0 to 2 degrees and where the charges of the essential bar were incorporated. A present integrator is utilized to quantify the aggregate charge episode on the essential focus all through the run.

The auxiliary pillar delivered from the essential response is gathered and centered in the diffusing chamber by utilizing a superconducting solenoid of the RIBRAS office. The particles with various attractive unbending nature were ceased from achieving the dispersing chamber after the solenoid utilizing an arrangement of squares and collimators. The normal power of the auxiliary shaft 8Li at the diffusing load was around 5 x 104 pps, which is ascertained by accepting unadulterated Rutherford scrambling of the 8Li on the gold target. Despite the fact that a few contaminants of 4He, 6He and 7Li were available in the auxiliary bar, they didn't create response items like the ones from our response. The 8Li research facility vitality was 19.6 MeV for the 9Be target, and 18.5 MeV for the 51V target. The estimations for the two frameworks were performed in ensuing runs. The versatile scattered response items with 8Li particles were recognized by a variety of four Si surface hindrance AE-E telescopes in a precise scope of 15-35 degrees in the lab framework, in 5 degree steps mounted on the pivoting plate of the chamber. The thickness of AE and E identifiers was 25 pm and 1mm, separately, both having a territory of 300 mm2. Rectangular collimators were likewise utilized before the identifier telescopes which subtended an edge of 12 msr for the meaning of strong points and to keep away from any scattered particles from the cuts. The objectives were mounted at the focal point of the diffusing chamber. The optional targets utilized were self-supporting, unadulterated 9Be, 51V focuses of thickness 1.4 mg/cm2 and 5 mg/cm2, separately. A gold focus of thickness 300 pg/cm2 was additionally utilized. The versatile dissipating of 8Li on this gold target was estimated in all keeps running at various points and used to get the general standardization.

Since the cross-areas in the precise interim secured by these indicators could fluctuate up to one request of greatness, the normal identification edge was controlled by Monte Carlo reenactments, which considered the collimator measure before the locators, the auxiliary bar spot estimate on the optional target (4 mm), the optional bar difference and the rakish conveyance in the scope of the finder opening (Rutherford on gold and figured in an iterative route for the 9Be target). This adjustment is essential for the most forward points. The compelling rakish opening of ±3.2 degrees was ascertained with a Monte Carlo recreation. Response items were recognized utilizing a two-dimensional AE-E add up to plot. Fig. 5.5 demonstrates a common 2D molecule distinguishing proof [C (Z, M) x Etotai] range for the 8Li on 9Be investigation at 19.6 MeV. Here, the molecule ID consistent, C (Z,M), is given by:

C (Z, M) = (Etotal)b-(Etotal - AE)b [33], (5.1)

where: Etotal = AE + Eresidualand b = 1.70 for these light particles. In this plot, the 8Li scattered shaft particles and the 4,6He pillar contaminants are appeared.

The optional pillar energies were ascertained by vitality misfortunes and affirmed by the vitality estimation in the Si telescope, adjusted with a-particles from a radioactive 241Am source and flexibly scattered auxiliary shafts. The FWHM of the versatile top in the vitality range was around 400 keV. The proportions of flexible diffusing rakish disseminations to the Rutherford dissipating for the Li + Be, at Elab = 19.6 MeV, and 8Li + 51V, at Elab = 18.5 MeV, are appeared in Figs. 5.6(a) and (b), separately.

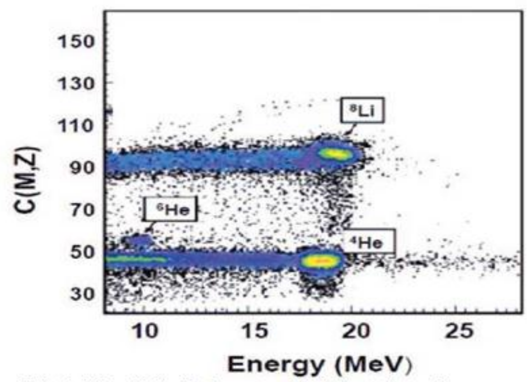

Figure 5.5. A typical 2D particle identification spectrum of the elastic scattering angular

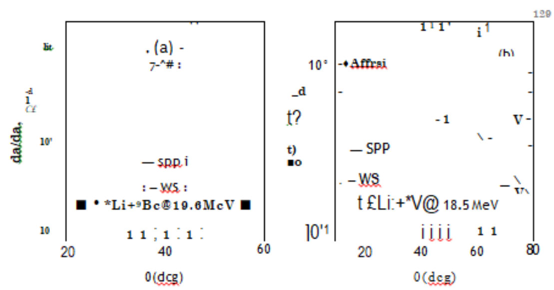

Figure 5.6. (a) Elastic scattering angular distribution for the Li + Be system at 19.6 MeV, 8 51 and (b) Elastic scattering angular distribution for the Li + V system at 18.5 MeV, measured in the present work. The solid line corresponds to best fit using the Sao Paulo potential (SPP) and the dashed line using the Woods - Saxon potential (WSP) form factors. See text for details.

Table 5.2. Barrier parameters obtained from the Sao Paulo potential (SPP) and derived total reaction cross-sections for the systems investigated in the present work. The crosssections obtained from data measured in the present work are in bold.

Sy stems	VB (MeV)	Rb (fm)	hoj (MeV)	Elab (MeV)	$X^2/n.$	0~T R (mb)
^{1g}O + °Be	5.19	8.15	2.44	15.0	0.45	187
				18.0	0.11	465
				21.5	0.16	742
				25.0	0.39	905
^{s}Li+ ^{9}Be	1.97	8.05	8.379	14.0	1.79	1267
				19.6	21.9	1332
				27.0	18.2	1370
^{r}Be + °Be	2.74	7.65	2.22	17.0	7.76	1060
				19.0	8.08	1116
				21.0	7.52	1197
^{7}Li + ^{c}Be	2.00	7.90	1.87	15.7	2.22	1323
				24.0	5.03	1365
				30.0	4.12	1414
^{G}Li+ ^{c}Be	2.04	7.72	2.00	4.0	0.78	358
				6.0	0.96	763
				32.0	2.93	1.082

Table 5.3. Barrier parameters obtained from the Sao Paulo potential (SPP) and derived total reaction cross-sections for the systems investigated in the present work. The crosssections obtained from data measured in the present work are in bold.

Sv steins	V_B (MeV)	Rb (fm)	Tuuj (MeV)	Elab (MeV)	X^2 in	(JTR (mb)
^{4} He + ^{51}V	7.49	8.20	3.93	23.2	1.0	1259
^{4}He + ^{56}Fe	8,38	8.30	4.08	25.0	28.0	1336
®He-f-^{si}V	6.61	9.25	2.72	15.4	0.9	1901
				23.0	0.4	2474
^{4} He + *^{4}Zn	9.50	8.45	4.31	13.0	0.8	585
				25.0	22.2	1365
^{G}Li + ^{GS}Ni	12.37	9.00	3.67	11.21	0.6	19
				12.13	0.1	40
				13.04	0.1	109
				14.04	0.3	225
				9.85	0.5	1.1
■Ce + $^{5\&}$Ni	16.59	8.95	3.91	15.09	0.1	21
				17.13	0.1	78
				18.53	0.1	193
				19.93	0.1	333
				21.43	0.1	499
^{s}B + ^Ni	20,80	8.92	4.09	20.7	0.15	198
				23.4	0.58	363
				25.3	0.33	512
				27.2	0.41	812
				29.3	0.13	1005
^{s}Li + ^{51}V	9.93	9.25	2.90	18.5	0.3	975
				26.0	1.5	1984

Optical model investigation of the flexible dispersing information

The optical model (OM) examination of versatile dissipating rakish conveyance information has been done to separate the optical potential parameters and response cross segments for all frameworks explored in this work. The potential utilized for all frameworks, aside from those with the radiance 6He and 8B, was the Sao Paulo twofold collapsing potential (SPP) [34]. The ECIS code [35] was utilized for the estimations. The genuine potential VN of SPP is identified with the collapsing potential VF by the connection,

$$V_N(R,E) = V_F(R)\exp\left(\frac{-4v^2}{c^2}\right), \qquad (5.2)$$

Where; u is the nearby relative speed between the two cores also, c is the speed of light.

The fanciful piece of the connection is accepted to have indistinguishable shape from the genuine part, with one single movable parameter Ni identified with its quality,

$$W(R, E) = N_i V_N(R, E), \qquad (5.3)$$

In the present estimation the customizable parameters taken were the quality parameters of the genuine and fanciful potential (Nr and N, separately). It has been indicated [36,37] that the examination of versatile dispersing rakish appropriations with SPP and with the phenomenological Woods-Saxon (WS) potential give similar outcomes for aggregate response cross-segments for firmly and no-radiance feebly bound frameworks, yet not for corona cores, attributable to the conduct of the potential at long separations, which is contradictory with the polarizations produced by the separation channels [38]. Therefore, for the frameworks including 6He and 8B investigated in the present work we utilized WS possibilities, rather than SPP. All things considered, to abstain from rehashing WS potential counts for the 8B+58Ni framework we took the response cross-area detailed prior [39] acquired by this system. For the 6He + 51V framework, just the profundities of the genuine and nonexistent possibilities were let to shift unreservedly in the fit technique. The diminished radii were settled in 1.2 fm for both the genuine and nonexistent piece of the potential and its diffuseness was taken equivalent to 0.7 fm and 0.9 fm, individually. Because of its inherent ambiguities, other optical potential parameters would give similar outcomes. We picked a bigger diffuseness for the nonexistent potential to represent the corona structure of the 6He shot.

The attacks of the flexible dispersing information estimated in the present work are appeared in Fig. 5.6. The inferred aggregate response cross-areas and hindrance parameters anticipated by the SPP for every one of the frameworks researched are appeared in tables 5.2 and 5.3. The main special cases are the response cross area including corona shots, for which the cross-segments were gotten utilizing the WS optical possibilities, as referenced previously. For alternate frameworks, tests were performed utilizing the two kinds of possibilities (as appeared in Figs. 5.6(a) and (b) for the information revealed in this work), and they prompt comparable aggregate response cross-areas.

Reduction technique of aggregate response cross area

With the end goal to play out a precise investigation of aggregate response cross-areas with various feebly bound shots with a few targets, it is important to contrast the cross segments for frameworks and distinctive Coulomb obstructions. For this reason, it is important to stifle the distinctions emerging from the size and charges of the frameworks. This should be possible in various ways. The two most much of the time utilized decrease systems are to standardize the crash vitality regarding the boundary tallness and to isolate the cross-segment by its geometrical esteem, i.e., to plot OR/TCR2B against Ec.m-VB or Ec.m./VB, where RB and VB are the s-wave obstruction sweep and stature separately, and ought to be assessed utilizing a practical treatment of the optical potential like the collapsing model. In any case, this technique does not consider the critical impact of the hindrance bend at the sub-obstruction energies [20]. It has been called attention to [19] that when pitifully bound shot cores are included, care ought to be taken with the end goal to save the static impacts emerging from the low separation vitality of the shot. In this way, the decrease technique evacuates the reliance on the majority and charges of the impact accomplices yet not explicit highlights of the 1/3 1/3 2 shot thickness. The proposed decrease strategy [19] is to plot oR/(Ap + A t) versus Ec.m.(Ap1/3 + A t13)/ZpZt. This strategy has been broadly used to examine the job of separation of pitifully bound cores on the combination and response cross-areas for an assortment of frameworks.

Be that as it may, it was as of late brought up [20] that the previously mentioned decrease techniques neglect to evacuate suitably the static impacts on the combination responses of various frameworks. In the recently proposed strategy [20], this is accomplished. This procedure was later reached out to be utilized with aggregate response cross-areas [13]. The system considers not just the stature and range of the Coulomb obstruction, yet additionally its ebb and flow spoken to by the amount hro. The impact vitality and the cross-segment are decreased, for combination cross-segments, as FF(x) = (2Ec.m./hroR2B)oF and x = (Ec.m. - VB) hro. So also, for aggregate response cross areas one uses FTR(x) = (2Ec.m./hroR2B) oTR. The hindrance parameters are extricated from the optical potential utilized. FF(x) was called combination capacity and FTR(x) was called add up to response work. It has been indicated [20] that this combination work is framework free when oF is precisely portrayed by Wong's recipe [48]. For this situation F(x) moves toward becoming F(x) ^ F0(x) = ln[1 + exp(2nx)]. Note that F0(x) depends solely on the dimensionless variable x. It is an all inclusive capacity which is the equivalent for any framework.

RESULTS

In Fig. 5.7 we think about aggregate response cross-areas for the 8Li + 9Be framework and the accessible aggregate response cross-segments for the 6,7Li + 9Be [49,50], 7Be + 9Be [51], 16O + 9Be [52] frameworks utilizing the two previously mentioned decrease techniques. We see that for all frameworks the objective is a pitifully bound core and the shots are either a firmly bound core or a feebly bound one yet not a corona core. The aggregate response cross-segments are in the vitality locale over the Coulomb boundary. In Fig. 5.7(b) we likewise demonstrate the UFF, as a source of perspective bend. One can see that the outcomes are comparative for every one of the frameworks when one diminishes the information by the two techniques. In this way, both decrease strategies prompt similar ends. The radioactive 8Li shot has the equivalent decreased aggregate response cross area as the stable 6Li isotope. One can see that the aggregate response cross-area for the firmly bound 16O shot is marginally littler than for the other feebly bound frameworks in Fig. 5.8(a), however not in Fig. 5.7(b), where all frameworks have add up to response cross-segments like the UFF. Comparable outcomes are available in refs. [13,21] for a comparative report with the 27Al target.

In Fig. 5.8 we look at aggregate response cross-areas for the 8Li + 51V framework and the accessible aggregate response cross-segments for the 4He + 51V [16], 6He + 51V [39], 4He + 56Fe [53], 4He + 64Zn [53-55], 6Li + 58Ni [39], 7Be + 58Ni [39], 8B + 58Ni [39] and 16O + 64Zn [56] frameworks utilizing a similar two decrease techniques. We see that the shots are either a firmly bound core or a feebly bound one, including the neutron corona 6He and the proton radiance 8B cores. Responses with the corona shots 6He and 8B have add up to response cross-areas higher than the others, autonomously whether they are firmly or pitifully bound cores, by both decrease strategies. 8Li has indistinguishable conduct from the stable 7Li isotope. By and by, the ends are the equivalent from both decrease strategies, despite the fact that the 16O shot shows littler aggregate response cross-area by the technique for Fig. 5.8(a). These ends are predictable with the ones acquired in ref. [13] for heavier frameworks. In that work, just aggregate response capacities initiated by neutron radiance (6He) and proton corona (8B) shots were bigger than for those incited by feebly or firmly bound cores.

For the information examined in the present work, both decrease methodology prompt similar ends. Notwithstanding, one must have at the top of the priority list that the frameworks researched here are not all that diverse having comparative result of the shot and target charges. By the decrease strategy for ref. [19] there is a pattern that heavier shots on a similar target have littler aggregate response cross-segments, as one can see in Figs. 5.8(a) and 5.9(a) for the 16O shot. It is as yet a matter of further examination which is the most ideal approach to

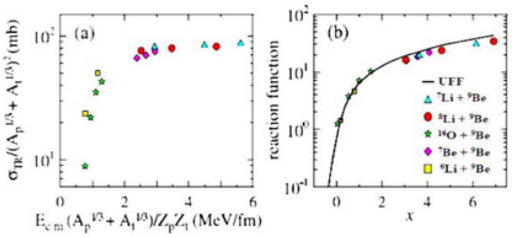

Figure 5.7. Total reaction cross-sections for systems with different projectiles and the same 9Be target, reduced by the two different reduction methods described in the text. The curve in (b) is the universal fusion function.

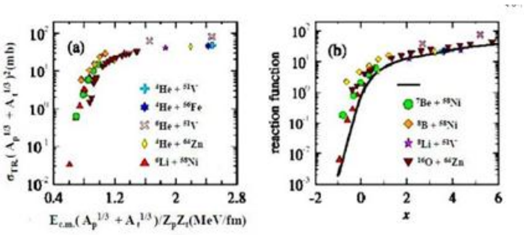

Figure 5.8. Total reaction cross-sections for systems with different projectiles and targets from A = 51 to 64, reduced by the two different reduction methods described in the text. The curve in (b) is the universal fusion function.

CONCLUSIONS

This part reports the new estimation of flexible scrambling cross-area for 8Li + 9Be and 8Li + 51V frameworks at 19.6 MeV and 18.5 MeV, separately, utilizing the radioactive bar office RIBRAS at Sao Paulo, Brazil. Investigations were performed for recently detailed information for these frameworks and for some other light frameworks. The twofold collapsing Sao Paulo potential was utilized in the examination everything being equal, aside from the ones with corona cores. In these cases, X fits and information investigation were performed utilizing Wood-Saxon shape optical possibilities. Tests were performed by utilizing the two sorts of possibilities for non-corona frameworks, and they prompt comparative aggregate response cross-segments, which were extricated from the optical model fits. The aggregate response cross-areas for all frameworks, and by the two decreasing techniques utilized, were observed to be comparative, regardless of the shot being firmly or pitifully bound, steady or radioactive, aside from when corona cores were available. In this circumstance, the aggregate response areas were bigger than for the others.

REFERENCES

1. W. Reisdorf, F. P. Hessberger, K. D. Hildenbrand, S. Hofmann, G. Munzenberg, K. H. Schmidt, J. H. R. Schneider, W. F. W. Schneider, K. Summerer, G. Wirth, J. V. Kratz, and K. Schlitt (2012). Phys. Rev. Lett 49, p. 1811.
2. D.M. Brink (2008). History of cluster structure in nuclei, Journal of Physics: Conference Series 111.
3. Prof. Martin Freer (2015). Ciusters in nuciei.
4. Taofiq Toyin Ibrahim (2009). A Cluster study of the nuclei 212Po and 218Rn, PhD, University of Stellenbosch.
5. A. Astier, P. Petkov, M.G. Porquet, D.S. Delion, and P. Schuck (2014). Novel Manifestation of a-Clustering Structures: New a + 208Pb States in 212Po Revealed by Their Enhanced E1 Decays.
6. S.L. Kakani and Shubhra Kakani : Nuclear and Particle Physics, Viva books private limited (ISBN: 978-81-309-0040-7).
7. S.N. Ghoshal, Nuclear Physics, S. Chand & company limited (ISBN: 81-219-0413-7).
8. K.H. Schmidt and W. Morawek (2014). Rep. Prog. Phys. 54, p. 949.
9. L.F. Canto, P.R.S. Gomes, R. Donangelo, M.S. Hussein (2006). Phys. Rep. 424, p. 1.
10. R. Raabe et. al. (2004). Nature 431, p. 823.
11. M. Kawai (1986). Prog. Theor. Phys. (Suppl.) 89, p. 11.
12. N. Austern et. al. (1987). Phys. Rep. 154, p. 125.
13. A. Diaz-Torres, I.J. Thompson (2002). Phys. Rev. C 65, p. 024606.
14. L.F. Canto, R. Donangelo, L.M. de Matos, M.S. Hussein (1998). P. Lotti, Phys. Rev. C 58, p. 1107.
15. M.S. Hussein, K.W. McVoy (2012). Nucl. Phys. A 445, p. 124.
16. M.S. Hussein, B.V. Carlson, T. Frederico, T. Tarutina (2004). Nucl. Phys. A 738, p .367.
17. M.A. Nagarajan, C.C. Mahaux, G.R. Satchler (2013). Phys. Rev. Lett. 54, p .1136.
18. G.R. Satchler (1991). Phys. Rep. 199, p. 147.
19. M E. Brandan, G.R. Satchler (1997). Phys. Rep. 285, p. 143.

20 N. Keeley et. al. (1994). Nucl. Phys. A 571, p. 326.

21. N. Keeley, K. Rusek (1997). Phys. Rev. C 56, p. 3421.

22. L.F. Canto et. al. (2009). J. Phys. G: Nucl. Part. Phys. 36, p. 015109.

23. E.A. Benjamim et. al. (2007). Phys. Lett. B 647, p. 30.

24. R. Lichtenth¨aler et. al. (2005). Eur. Phys. J. A 25, s01, p. 733.

25. R. Lichtenth¨aler et al., AIP Conf. Proc. 1139, 76 (2009).

26. F.D. Becchetti et. al. (1993). Phys. Rev. C 48, p. 308.

27. G.F. Knoll (1989). Radiation Detection and Measurement (Wiley & Sons, New York, 1989) p. 380.

28. L.C. Chamon et. al. (2012). Phys. Rev. C 66, p. 014610.

29. J. Raynal (1981). Phys. Rev. C 23, p. 2571.

30. J.M. Figueira et. al. (2016). Phys. Rev. C 73, p. 054603.

31. J.M. Figueira et. al. (2007). Phys. Rev. C 75, p. 017602.

32. A.R. Garcia et. al. (2008). Nucl. Phys. A 806, p. 146.

33. E.F. Aguilera et. al. (2009). Phys. Rev. C 79, p. 021601(R).

34. A. Barioni et. al. (2009). Phys. Rev. C 80, p. 034617.

35. F.A. Souza et. al. (2009). Nucl. Phys. A 821, p. 36.

36. U. Gupta et. al. (2008). Nucl. Phys. A 811, p. 77.

37. A. Di Pietro (2007). Eur. Phys. J. ST 150, p. 15.

38. M. Sinha et al. (2007) Phys. Rev. C 76, p. 027603.

39. K. Kalita et al. (2006). Phys. Rev. C 73, p. 024609.

40. E.F. Aguilera, J.J. Kolata, L. Acosta (2010). Phys. Rev. C 81, p. 011604(R).

41. M. Mazzocco et al. (2010). Nucl. Phys. A 834, p. 488c.

42. C.Y. Wong (1973). Phys. Rev. Lett. 31, p. 766.

Corresponding Author

Deepak Saini*

Research Scholar of OPJS University, Churu, Rajasthan